Haptic Feedback and the Internal Model Principle

Steven Cutlip[1], Jim Freudenberg[2], Noah Cowan[3], and R. Brent Gillespie[1]

***Abstract*— According to the internal model principle from control engineering, error feedback together with a controller containing an internal model that generates an expected disturbance signal can achieve perfect delay-tolerant disturbance rejection using only modest loop gains. While internal models of plant dynamics have been central to the study of human motor control, internal models of reference or disturbance signal generators have received very little attention. In this paper we show how the internal model principle suggests a certain control strategy for achieving steady oscillatory motion in a virtual spring-mass. The strategy relies on haptic feedback in its dual roles of carrying power and information and this dual reliance may be used to derive numerous testable hypotheses. We present results from an initial study involving N=5 human subjects in which high time-correlation between surface electromyography and commanded torque signals suggests the adoption of a control strategy based on the internal model principle.**

I. INTRODUCTION

When haptic feedback is denied, performance in most manipulation tasks degrades significantly, often failing altogether. Thus we know that haptic feedback informs control strategies used to assess mechanical properties, to identify and sort objects, to guide manipulation processes, and to tune motor control strategies. But how exactly does the human motor system make use of haptic sensory feedback? Naturally, haptic feedback across a mechanical contact carries not only sensory information but also mechanical power. How does the motor control system make sense of these intertwined roles? These questions are of high interest for scientific reasons and to inform the design of control algorithms for autonomous robots, for robots that work cooperatively with humans, and for robots designed to train or rehabilitate human motor skill.

Juggling is a manipulation skill that has garnered significant study from the perspective of control, robotics, and computational neuroscience. It has been found that haptic feedback is critical to stabilize and maintain a steady juggling height [1], [2]. A continuous system counterpart to juggling without discrete contacts is eliciting and maintaining oscillation in a mechanical oscillator. Examples of mechanical oscillators include a torsional spring-inertia system as shown in Fig. 1. The value of haptic feedback for eliciting oscillations in a spring-mass has been studied from an empirical standpoint in [3]. Huegel and O'Malley used the challenge of maintaining oscillations at a specified amplitude as a task to be trained with haptic guidance [4]. Dingwell et al. [5] observed sophisticated model-based strategies for moving a mass from an initial to final rest position through a spring.

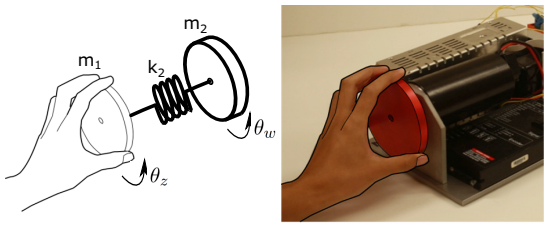

Fig. 1. When rendered through a haptic device, a virtual torsional spring of stiffness K and inertia J_M can be used to study manipulation tasks akin to juggling.

The internal model principle, a tenet in control engineering since the early 1970s [6], states that a feedback controller containing a model of the signal to be tracked or rejected (exogenous signals) can achieve, using only modest loop gains, perfect reference tracking or disturbance rejection. A model in the controller acts to generate the signal that precisely zeros out the error between desired and actual system response. The internal model principle generalizes the manner in which integral control eliminates static steady-state error (the zero response of an integrator with a non-zero initial condition). Thus, to track a persistent sinusoidal reference at frequency ω_0, the internal model principle posits that the controller should contain poles at $s = \pm j\omega_0$. In steady state, this controller will generate the excitation that produces perfect reference tracking.

The internal model principle has its adherents in engineering practice, most notably in the disk drive industry [7]. However, as a hypothesis for biological control, the internal model principle has found very little exploration to date with the exception of [8]. Contrast this unexplored territory to the use of internal models of plant dynamics (endogenous system), which has produced a very large literature [9]–[11]. Also not that the internal model principle does not propose an *inverse model* in a feedforward controller (where it would be useful for cancelling plant dynamics). Instead, the internal model principle proposes that a model of the expected reference or disturbance signal generator be placed in the control loop.

In this paper we use the internal model principle to generate hypotheses about human control strategies for driving oscillations in an undamped spring-mass system. We account for the dual roles of haptic feedback for power

[1]Mechanical Engineering, University of Michigan, Ann Arbor, USA scutlip@umich.edu,brentg@umich.edu

[2]Electrical Engineering and Computer Science, University of Michigan, Ann Arbor, USA jfr@umich.edu

[2] Mechanical Engineering, Johns Hopkins University, Baltimore, MD, USA ncowan@jhu.edu

This work was carried out under support from the National Science Foundation, grant No. 1825931.

and information exchange in our system models (section II) and undertake a human participant study to test the predictions produced by hypothesizing a neural controller based on the internal model principle (sections III and IV). We conclude by observing that the internal model principle gives a parsimonious explanation of how humans use haptic feedback to perform cyclic manipulation tasks.

II. Model Development

Due to compliance in muscle, the body's dynamics are liable to become coupled to the dynamics of objects being manipulated, especially when the impedance of the body and object are approximately matched. In such case the nervous system is faced not with the control of the object dynamics, but with the control of the coupled dynamics of body and object. Even in producing desired motions in a simple mass, it is necessary to devise a strategy that will arrest both the kinetic and potential energy in the coupled dynamics of body and mass. In essence the human motor system solves the crane operator's problem even when moving a rigid object, so long as the inertia forces produce extensions in muscle [12]. All the while it may not "feel" like a sophisticated strategy, given that proprioception and force sensing is available at the hand, that distal attribution is likely at play [13], and that the brain's schemes may not be available for introspection.

Note that driving-point impedance can be modulated by co-contracting muscles or changing posture. Thus one might choose to eliminate compliance from the manipulation challenge by co-contracting muscles. However, such a strategy is generally reserved for the early stages of motor learning [14]. Studies have shown that humans prefer to adopt a modest compliance and a more sophisticated control strategy in the latter stages of learning [5] to save energy and increase performance.

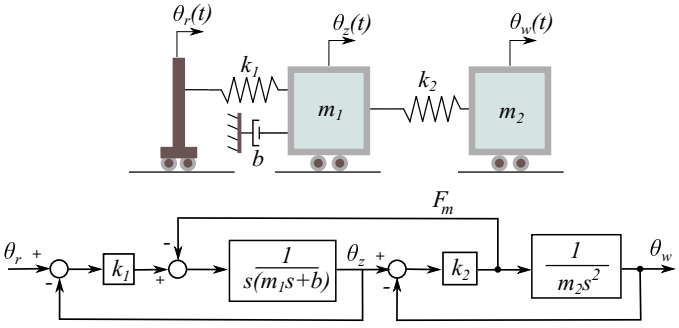

Fig. 2. The compliance of muscle encapsulated in stiffness k_1, along with damping b and mass m_1 that describe the backdrive impedance of the body, are driven by a motion source $\theta_r(t)$ to produce displacements $\theta_z(t)$ at the hand. The dynamics of an oscillator comprising stiffness k_2 and mass m_2, when rendered through the haptic device with force F_m, become coupled to the dynamics (biomechanics) of the body. By linearity, a persistent sinusoidal excitation $r(t)$ at frequency $\omega_0 = \sqrt{k_2/m_2}$ will produce, at steady-state, a sinusoid at $\omega_0 = \sqrt{k_2/m_2}$ in $\theta_w(t)$ and $\theta_z(t) \to 0$. Note: transitional diagram is standing in for what might be a rotational system

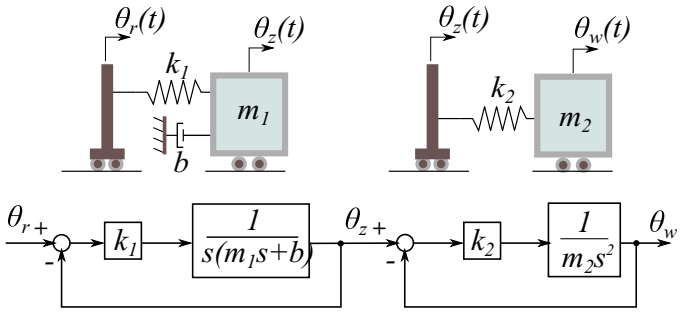

Fig. 3. Without coupling, or if the haptic device motor is disabled, the dynamics of the virtual spring-mass system is driven by the motion source $\theta_z(t)$, the displacement of the haptic device handle.

A. Open Loop Strategies For Driving Oscillations

Consider now the manipulation of a non-rigid object like a spring-mass (without damping). And suppose the manipulation challenge is to maintain sustained oscillations in this mechanical oscillator. Given that a distal mass is part of the model for the driving point impedance of the hand [15]–[17], when the dynamics of a spring-mass are coupled to the body, a system with fourth-order dynamics results. Figure 2 shows a mass m with displacement $\theta_z(t)$ along with stiffness k_2 and damping b that describes the driving point impedance at the hand. This second order driving point impedance is elaborated with a motion source $\theta_r(t)$ to describe volitional muscle action [17]. Figure 2 also shows the same model in the form of a block diagram, where the role of the force F_m carried in the spring K becomes apparent as a feedback path coupling the dynamics of the undamped oscillator with the dynamics of the body. The response of hand displacement $\theta_z(t)$ and oscillator displacement $\theta_w(t)$ to an excitation $\theta_r(t)$ may be obtained directly from the block diagram:

$$\frac{\theta_Z(s)}{\theta_R(s)} = \frac{G(s)}{1 + \frac{m_2}{k_2} s^2 G(s) H(s)} \tag{1}$$

$$\frac{\theta_W(s)}{\theta_R(s)} = \frac{G(s)H(s)}{1 + \frac{m_2}{k_2} s^2 G(s) H(S)}, \tag{2}$$

where $G(s) = \frac{k_1}{m_1 s^2 + bs + k_1}$ and $H(s) = \frac{k_2}{m_2 s^2 + k_2}$.

To make the poles and zeros of these transfer functions explicit, let us express $G(s)$ as a ratio of polynomials $\frac{b_G(s)}{a_G(s)}$ and $H(s)$ as $\frac{\omega_0^2}{(s^2+\omega_0^2)}$ (highlighting the undamped oscillator dynamics with natural frequency $\omega_0 = \sqrt{k_2/m_2}$). Then the transfer functions in Eqs. 1 and 2 can be re-written:

$$\frac{\theta_Z(s)}{\theta_R(s)} = \frac{b_G(s)(s^2 + \omega_0^2)}{a_G(s)(s^2 + \omega_0^2) + \frac{m_2 \omega_0^2}{k_2} s^2 b_G(s)} \tag{3}$$

$$\frac{\theta_W(s)}{\theta_R(s)} = \frac{\omega_0^2 b_G(s)}{a_G(s)(s^2 + \omega_0^2) + \frac{m_2 \omega_0^2}{k_2} s^2 b_G(s)}. \tag{4}$$

Note that the poles of $H(s)$ appear as zeros in the transfer function $\frac{\theta_Z(s)}{\theta_R(s)}$. See also the Bode plot in Fig. 4(A). These are called transmission zeros, and they suggest the following control strategy to achieve sustained oscillations in the oscillator: Simply excite the coupled dynamics with

a sinusoid at frequency ω_0. Given that $\frac{\theta_W(s)}{\theta_R(s)}$ is stable and linear, the steady-state response $\theta_w(t)$ to $\theta_r(t) = \sin\omega_0 t$ will be a sinusoid at ω_0 with possibly a different amplitude and phase. At the same time $\theta_z(t) \to 0$, precisely because of the presence of the transmission zeros in $\frac{\theta_Z(s)}{\theta_R(s)}$.

Note that the discussion so far also pertains to the manipulation of a virtual spring-mass rendered through a haptic device. The mass m_1 and damping b modeling human impedance may alternatively be lumped with the physical dynamics of a haptic device. Also, whether the damper b links mass m_1 to ground or to the motion source $r(t)$ is immaterial to the arguments that follow.

What would be the behavior of the spring-mass oscillator without haptic rendering (if the haptic device motor were turned off)? When $F_m(t) = 0$, the user and spring-mass are no longer mechanically coupled, as shown schematically in Fig. 3. Information flows, in that the motion source $\theta_z(t)$ driving the virtual spring-mass is derived from the instrumented haptic wheel. But mechanical power is no longer exchanged across the haptic device. In this case the response $\theta_z(t)$ to a persistent sinusoidal excitation $\theta_r(t) = \sin\omega_0 t$ is given by $\theta_Z(s) = G(s)\theta_R(s)$ from which we see that the steady-state response $\theta_z(t)$ is a sinusoid at frequency ω_0 (see Fig. 4B). In turn, the spring-mass responds with an oscillation whose amplitude grows without bound.

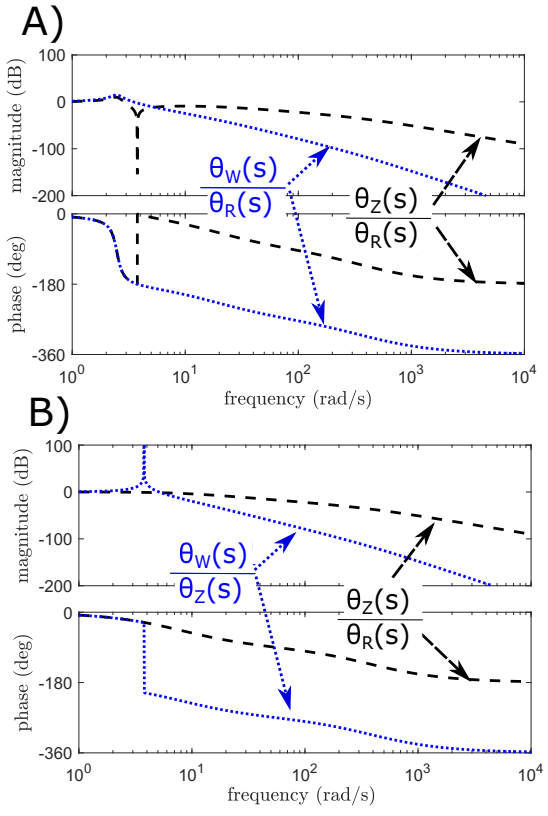

Fig. 4. (A) The coupled system displays a null response in the response of θ_z and a steady response in θ_w to sinusoidal excitation in θ_r at $\omega_0 = 0.6$ rad/s. (B) The uncoupled system, on the other hand, displays a steady response in θ_z and an unstable response in θ_w.

Let us compare the control strategies available to a human user attempting to maintain steady oscillations in the virtual spring-mass in the cases of coupled and uncoupled dynamics (with and without haptic rendering). For the case of coupled dynamics, the smooth amplitude function $\frac{\theta_W(s)}{\theta_R(s)}$ in Fig. 4A serves as a map to select an amplitude for an open-loop strategy based on generating a persistent sinusoidal control input. The map can also be applied at frequencies other than ω_0. Note that this strategy is very robust and even insensitive to loop delays because it is, after all, an open-loop strategy. In that sense it may be considered a feed-forward control strategy. Note that this feedforward strategy does not make use of an inverse model of the spring-mass system, as in standard conceptions of model-based feedforward control [9].

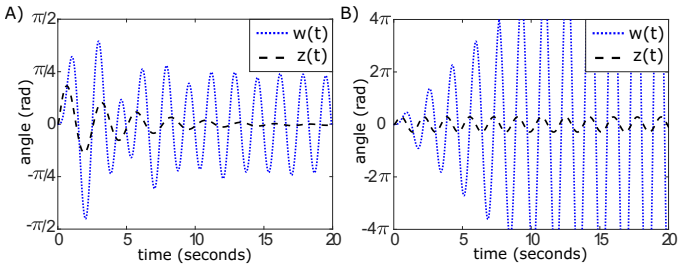

Fig. 5. Time domain simulation results. (A) Coupled system, (B) Uncoupled system. Parameter values were selected as follows: $k_1 = 2.1$ N/m, $b = 0.27$ Ns/m, $m_1 = 0.00068$ kg, $m_2 = 0.2$ kg, $k_2 = 2.84$ N/m.

B. Closed Loop Strategies For Driving Oscillations

What is available to the user if feedback is added to the open-loop strategy for the control of the coupled dynamical system described above? After all, haptic feedback is available as a neural signal, provided to the central nervous system by haptic sensory organs. We can now ask how closed-loop sensory feedback might enhance performance and additionally whether a feedback strategy would be sensitive to the loop delays inherent in human motor control.

We presume that a neural substrate is available to generate a sinusoidal command to muscle at a specified frequency and amplitude (this is represented in Fig 6 as the block $C(s) = C_0/(s^2 + w_0^2)$ which describes a sinusoid at frequency w_0 in the laplace domain). We also suppose that there exists a means of generating a signal $F_m^{exp}(t)$ that describes the expected haptic feedback, or the force $F_m(t)$ felt by the hand grasping the haptic device. An error signal $e(t)$ could be formed by computing the difference between the expected and actual haptic feedback, as shown in the block diagram in Fig. 6A. An analysis of this loop shows that $\frac{E(s)}{F_m^{exp}(s)}$ also has transmission zeros at the roots of $(s^2 + \omega_0^2)$.

Again it follows that $e(t) \to 0$ for $F_m^{exp}(t) = \sin\omega_0 t$. Figure 7 shows results from a simulation of an internal model controller C(s) closing a loop around the coupled system. C(s) is simply a model or generator of steady oscillations characteristic of the spring-mass. When driven with $F_m^{exp}(t) = A_d \sin(\omega_0 t + \phi_d)$, where A_d and ϕ_d are

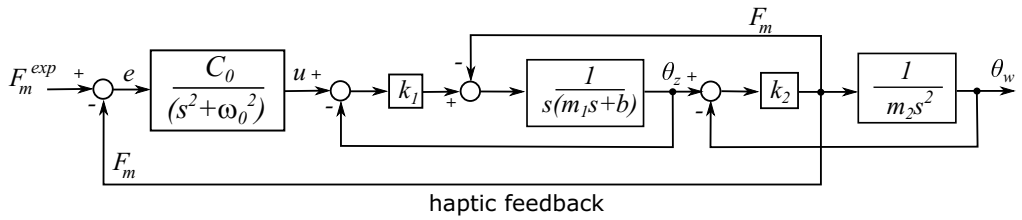

Fig. 6. Block diagrams for the closed-loop controller based on the internal model principle wrapped around the coupled system

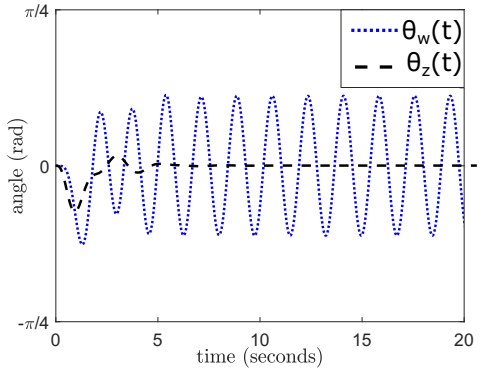

Fig. 7. Time domain simulation results for the closed-loop system shown in Fig. 6. The value 1 was used for the single free controller parameter C_0.

a desired amplitude and phase, this controller will produce, after a brief transient, steady oscillations in the virtual spring-mass system with $z(t) \to 0$ (haptic device handle motionless) and $e(t) \to 0$. That is, all objectives are achieved: $\theta_W(t) = A\sin(\omega_0 t + \phi)$, with $A \to A_d$ and $\phi \to \phi_d$.

The control strategy based on the internal model principle described above is also compatible with an adaptive controller that supports adjustment in control parameters C_0 or ω_0. Whether the neural substrates are available to support the computations suggested in the block diagram of Figure 6 or some alternate computation produces similar behavior remains an open topic. In the meantime, we undertake a human participant study to test some of the hypotheses generated by the exposition above.

In our human subject experiment we evaluated three strategies "Relax", "Co-contract", and "Oppose" with the expectations that follow from our analysis above. First, we expect that oscillations in the coupled dynamics will decay in amplitude if the user relaxes their muscles ("Relax" strategy). A second approach to maintaining oscillations is co-contracting muscles (increasing impedance) in an attempt to hold the handle stationary ("Co-contract strategy"). In such case muscle action will be high and steady, not correlated to the sinusoidal motion of the oscillator. Both of these strategies do not correspond to diagram 6 because the neural substrate is not generating a sinusoid. These strategies are better understood by viewing figure 2 where the strategy of relaxing corresponds to the human maintaining nominal k_1 and b and the strategy of co-contracting corresponds to increasing k_1 and b such that the human acts like a high gain position controller. Alternatively, the user may adopt the approach, we will call "Oppose", suggested by the internal model principle: to simply balance the force feedback felt from the haptic device. Our analysis suggests that this strategy will also eliminate motion in the haptic device, resulting in sustained oscillations in the virtual spring-mass. This balancing the force feedback is what is shown in 6. It is important to note here that for all three strategies the transfer function shown in eq(4) is representative of all three cases of the coupled human wheel system and these strategies simply represent a construction of θ_r (in the case of "Oppose") or adjustments to b and k_1 (in either "Relax" or "Co-contract").

III. Methods

A. Participants and Apparatus

Experiments were conducted with 5 participants (3 male, 2 female) from the population of engineering students at the University of Michigan. All participants signed an informed consent according to an IRB approved protocol (HUM00148462). The angular position θ_Z of the haptic wheel (Encoder - US Digital E6S-2048-157), the angular position θ_W of the virtual wheel, an amplified, rectified measure EMG of surface electromyographic signal (Ottobock $13E200 = 60$) from the medial aspect of the forearm, and the current commanded to the motor (Maxon $RE-40-148877$) were all recorded at 1KHz. The EMG signal was low pass filtered at 5Hz. All signals were collected using a Sensoray 626 and Simulink real-time at 1KHz. The haptic wheel is pictured in Fig. 1.

B. Experiment Conditions

Each participant was instructed to grasp the haptic wheel, which was rendering a virtual spring-mass with a natural frequency f_n = 0.6Hz. A diagram of the coupled system is shown in Fig. 2. The participant was asked to displace θ_Z by about 160°), return θ_Z to 0° to excite the system, and then attempt to maintain oscillations under three instructions: "Relax", "Co-contract", and "Oppose". The instructions under the "Relax" were to passively hold the wheel. Under "Co-contract", the participants were asked to hold the haptic wheel stationary at 0° by contracting their arm muscles hard (holding the haptic wheel stiffly). In the "Oppose" strategy the instructions were to counteract the torque they felt by applying an opposing torque that would keep the wheel steady at about 0°. The duration of each trial was 120 seconds.

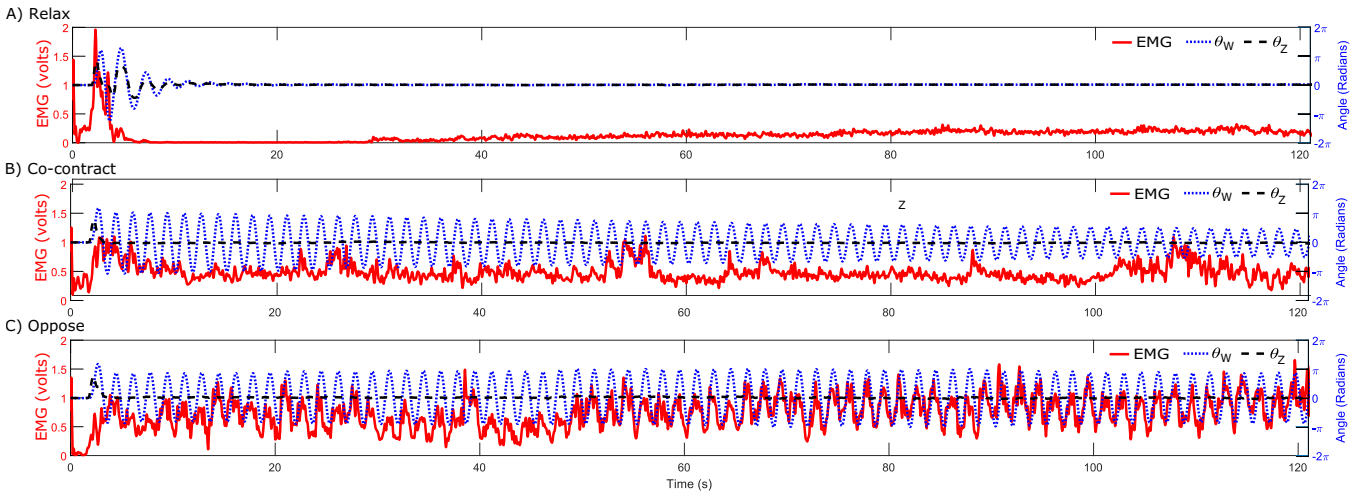

Fig. 8. Raw Signals: EMG, Virtual Wheel θ_w, and Physical Wheel θ_z position for Participant 4 (S4). The force F_m experienced by the user is proportional to the difference between θ_w and θ_z

IV. Results

A. Raw Signals

The raw signals for a sample participant (S4) are shown in Fig. 8 including EMG, the physical wheel position θ_z, and virtual wheel position θ_w under all three control strategies. The oscillations decay rapidly under "Relax", decay slowly under "Co-contract", and are maintained (or only decay slightly) under "Oppose".

B. Fast Fourier Transform (FFT)

A single sided FFT from one subject (S4) is shown in Fig. 9 where a spike in the EMG signal present at the natural frequency (0.6 Hz) can be seen in the "Oppose" strategy and is not present in either the "Relax" or "Co-contract" strategies. Both the "Co-contract" and "Oppose" strategies have a large DC component (near $f = 0$). The oscillations in θ_W were successfully generated at 0.6 Hz in the case of the "Co-contract" and "Oppose" conditions, whereas oscillations were not generated in the "Relax" strategy. The relax strategy does however have a smaller spike closer to $0.45Hz$ due to the dampened oscillations that were seen in Fig. 8. The powers in both the EMG and θ_W time signals at the natural frequency for all participants are shown in Table I. I.

C. Signal Energy

To compare differences in the amount of control effort, the energy of the EMG and θ_W signals was calculated in all conditions, and can be seen in Table I. It is evident that the Energy in "Co-contract" and "Oppose" conditions is typically higher than "Relax", as expected. In addition, the energy in "Co-contract" is about twice that of the "Oppose" condition showing that the "Co-contract" strategy requires considerably more control effort.

D. Phase Plots

For each participant and strategy the derivative $\frac{d\theta_W}{dt}$ was calculated and plotted against θ_W as a function of time. The trajectories start at $(0, 0)$, spiral quickly outwards due to the large initial excitation, and then either spiral back towards $(0, 0)$ or maintain a circular oscillatory pattern. In figure 10 the phase plots calculated in this manner are shown for all participants and strategies. The "Relax" strategy trajectories quickly decay, the "Co-contract" trajectories decay slowly, and the "Oppose" trajectories decay slightly but are the best maintained. The differences between subjects during these conditions have to do with each subject having differing m_1, k_1, and b parameters as well as differing success in performing the control task. The take away from these results is all of the human subjects performed similarly in terms of general behavior. The one apparent difference is that S3's oscillations are large and tend to spiral outwards. This is likely due to S3 injecting energy into the system by having too large an input command; driving the system instead of just compensating for the haptic feedback.

		0.6Hz Peak		Signal Energy	
		EMG	θ_W	EMG	θ_W
S1	A) Relax	0.004	0.014	0.003	0.103
	B) Co-contract	0.269	1.928	2.577	3.226
	C) Oppose	0.395	3.959	1.097	8.462
S2	A) Relax	0.020	0.011	0.149	1.861
	B) Co-contract	0.478	1.377	1.983	1.219
	C) Oppose	0.833	2.339	1.695	3.223
S3	A) Relax	0.006	0.073	0.015	0.455
	B) Co-contract	0.291	5.903	1.567	23.94
	C) Oppose	0.194	9.950	1.982	163.2
S4	A) Relax	0.002	0.039	0.037	0.197
	B) Co-contract	0.022	1.780	0.235	2.350
	C) Oppose	0.183	2.235	0.632	3.927
S5	A) Relax	0.002	0.023	0.004	0.943
	B) Co-contract	0.130	1.994	0.573	2.359
	C) Oppose	0.108	2.089	0.234	4.534

TABLE I

Power at 0.6 Hz and signal energy associated with EMG and θ_W for all three strategies and all 5 participants.

V. Discussion and Conclusion

The correlation between surface EMG signals and virtual oscillator displacement was evident when our participants held the haptic device stationary by opposing the torque that

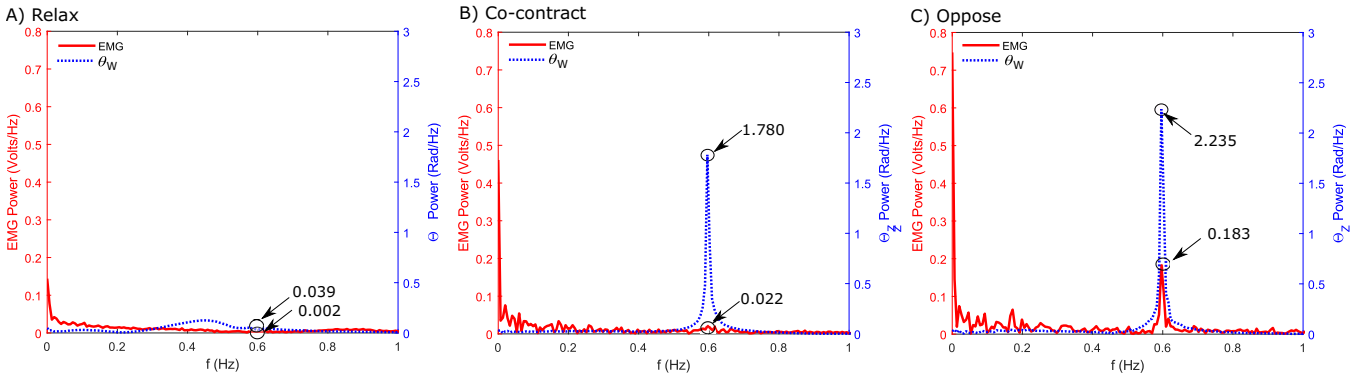

Fig. 9. Fast Fourier Transforms: EMG and Virtual Wheel Position for Subject 4 (S4)

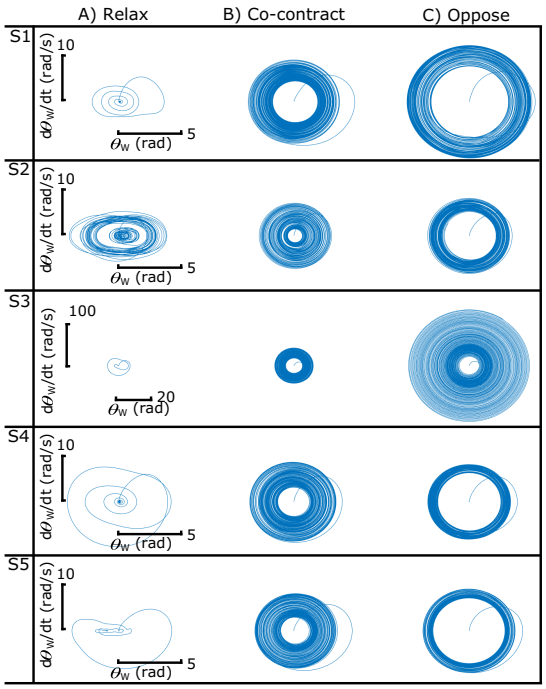

Fig. 10. In this figure $d\theta_W/dt$ is plotted against θ_W for all three strategies and all 5 participants creating phase plots.

they felt. However, this cannot be taken as direct evidence of a neural controller containing a sinusoid generator per the internal model principle. But the alternative hypothesis involving the formation of an error using (delayed) haptic feedback would by comparison be very sensitive to parameter perturbations and noise. Our results also show that an approach involving increased impedance, which can either be construed as brute force quelling of haptic device motion or high gain error feedback on haptic device displacement, was by comparison a more costly approach. By making this energy comparison we are pointing out that a human's innate ability to make predictions and interpret haptic feedback naturally allows for energy conservative strategies for movement. It should also be noted that the arm model we used in this work is a simplistic approximation. For future work a more complex nonlinear model with more degrees of freedom could be explored. We are also interested in looking at better separating feed forward, feedback, and internal model principle elements of human motor control, the effects of varying haptic feedback, and the effects of varying preview.

References

[1] S. Schaal and C. G. Atkeson, "Open Loop Stable Control Strategies for Robot Juggling," in *IEEE International Conference on Robotics and Automation*, vol. 3, 1993, pp. 913–918.

[2] M. M. Ankarali, H. Tutkun Sen, A. De, A. M. Okamura, and N. J. Cowan, "Haptic feedback enhances rhythmic motor control by reducing variability, not improving convergence rate," *Journal of Neurophysiology*, vol. 111, no. 6, pp. 1286–1299, 2014. [Online]. Available: http://jn.physiology.org/cgi/doi/10.1152/jn.00140.2013

[3] F. Huang and R. B. Gillespie, "Haptic Feedback and Human Performance in a Dynamic Task," in *10th Symp. On Haptic Interfaces For Virtual Envir. & Teleoperator Sys.*, 2002.

[4] J. C. Huegel and M. K. O'Malley, "Progressive haptic and visual guidance for training in a virtual dynamic task Progressive Haptic and Visual Guidance for Training in a Virtual Dynamic Task," in *IEEE Haptics Symposium*, 2010, pp. 343–350.

[5] J. B. Dingwell, C. D. Mah, and F. A. Mussa-ivaldi, "Experimentally Confirmed Mathematical Model for Human Control of a Non-Rigid Object," *Neurophysiology*, vol. 91, pp. 1158–1170, 2019.

[6] B. A. Francis and W. M. Wonham, "The Internal Model Principle of Control Theory," *Automatica*, vol. 12, no. 5, pp. 457–465, 1976.

[7] X. Guo and M. Bodson, "Equivalence between adaptive feedforward cancellation and disturbance rejection using the internal model principle," *International Journal of Adaptive Control and Signal Processing*, vol. 24, no. April 2009, pp. 211–218, 2010.

[8] J. Huang, A. Isidori, L. Marconi, M. Mischiati, E. Sontag, and W. M. Wonham, "Internal Models in Control, Biology and Neuroscience," *Proceedings of the IEEE Conference on Decision and Control*, vol. 2018-December, no. Cdc, pp. 5370–5390, 2019.

[9] D. M. Wolpert, R. C. Miall, and M. Kawato, "Internal models in the cerebellum," *Trends in Cognitive Sciences*, vol. 2, no. 9, pp. 338–347, 1998.

[10] M. Kawato, "Internal models for motor control and trajectory planning Mitsuo Kawato," *Current Opinion in Neurobiology*, pp. 718–727, 1999.

[11] R. C. Miall and D. M. Wolpert, "Forward Models for Physiological Motor Control," *Neural Networks*, vol. 9, no. 8, pp. 1265–1279, 1996.

[12] T. Yamashita, T. Nakamura, M. Ohtsuka, and T. Taniguchi, "HEURISTIC LEARNING PROCESS OBSERVED IN MANUAL CONTROL OF CRANE," *IFAC Proceedings Volumes*, vol. 14, no. 2, pp. 1041–1046, 1981. [Online]. Available: http://dx.doi.org/10.1016/S1474-6670(17)63618-8

[13] M. Loomis and S. Barbara, "Distal Attribution and Presence," *Presence*, vol. 1, no. 1, 1991.

[14] E. Burdet, R. Osu, and D. W. Franklin, "The central nervous system stabilizes unstable dynamics by learning optimal impedance," *Nature*, vol. 414, no. November, 2001.

[15] C. J. Hasser and M. R. Cutkosky, "System Identification of the Human Hand Grasping a Haptic Knob," in *10th Symp. On Haptic Interfaces For Virtual Envir. & Teleoperator Sys.*, 2002.
[16] A. Hajian and R. D. Howe, "Identification of the Mechanical Impedance at the Human Finger Tip," *Journal of Biomechanical Engineering*, vol. 119, no. February 1997, pp. 109–114, 1997.
[17] B. Yu, R. B. Gillespie, J. S. Freudenberg, and J. A. Cook, "Identification of Human Feedforward Control in Grasp and Twist Tasks," in *2014 American Control Conference*, 2014, pp. 2833–2838.